# Original Research Article
# Study of aerosol impact on the solar potential available in Burkina Faso, West Africa

**Bado Nébon[1,2*], Mamadou Simina Dramé[2], Korgo Bruno[1], Guengane Hassime[1], Demba Ndao Niang[2], Saidou Moustapha Sall[2], Kieno P. Florent[1], Bathiebo Dieudonné Joseph[1]**

*[1]Laboratoire d'Energies Thermiques Renouvelables (L.E.T.RE), Université Ouaga I Pr Joseph KI ZERBO, BP 13495 Ouaga, Burkina Faso*

*[2]Laboratoire de Physique de l'Atmosphère et de l'Océan Siméon-Fongang, Université Cheikh Anta DIOP, BP 5085 Dakar-Fann, Sénégal*

REVIEW

## ABSTRACT

This paper is an assessment of aerosols impact on solar potential available in Burkina Faso in 2017. Three measurement stations were selected from the North to the South according to the climatic zones, with sites at Dori (14.035 °N, 0.034°W) in the North, Ouagadougou (12.20°N, 1.40°W) in the Center and Gaoua (10.29°N, 3.25°W) in the Southwest, respectively. This study is based on in-situ measurements, satellite observations and a tropospheric standard model of the Streamer radiative transfer code of atmospheric particles. The results show a high availability of solar irradiation with average monthly values ranging between 4.46 kWh/m²/d and 6.82 kWh/m²/d. The most favorable periods with maximum radiation are observed in Spring in March and in Fall in October. Yet, the qualitative comparison between the evolution of aerosols and that of solar potential clearly shows aerosols capacity to influence the radiation at the crossing of the atmosphere. Thus, the aerosols maxima correspond to the solar potential minima. Moreover, a comparison between the day cycles of solar radiation and those of the simulation model shows a good accuracy of the Streamer code to estimate the solar flows at the surface in a standard atmosphere without clouds in Burkina Faso. However, a quantification of the aerosol impact by the Streamer code reveals a reduction in the normal direct flow compared to clear days defined by aerosol optical depth (AOD) less than 0.2 (AOD < 0.2) of nearly 75.04% at the Dori site in the North, 57.33% at the Ouagadougou site in the Center and 40.89 % at the Gaoua site in the Southwest during polluted days corresponding to AOD higher than 0.8. This corresponds to an increase in the diffuse flow of 279.69 W/m², 246.05 W/m² and 226.09 W/m², respectively calculated on the same sites. In case of a mixed day (0.2 <AOD <0.8), this decrease in direct solar flow is estimated at 41.25%, 22.11% and 37.13% with an increase in the diffuse solar flux of 115.04 W/m², 150.43 W/m² and 79.58 W/m² at the sites of Dori, Ouagadougou and Gaoua, respectively.

***Keywords*** *: Aerosols, Solar potential, Model Streamer, MODIS, AERONET, Burkina Faso*

** Corresponding author: E-mail address: nebonbado@gmail.com*

## 1. INTRODUCTION

West Africa, particularly the Sahel region, is one of the main high potential areas in terms of dust sources and combustion aerosols in the world [1, 2]. In West Africa, aerosols are strongly influenced by mineral dust because this zone is close to the Sahara, which is recognized as the first source of dust emissions, with a surface area of nearly 8.5 million $km^2$. Like the desert dust, there are also biomass combustion products (wood burning, bush fires, fuels) whose main sources are located in the Gulf of Guinea in the south of Burkina Faso [1]. As a result, dust clouds spread regularly across the continent and to the ocean, notably in Winter and Spring [3, 4]. These mineral dusts have strongly influence the radiative balance, the climate and also affect the hydrological cycle [5, 6, 7]. In addition, an analysis of in-situ measurements of the AERONET (AErosol RObotic NETwork) network made by Dramé et al [8] makes it possible to locate aerosol maxima in West Africa in Spring (March-April-May) and in Summer (June-July-August) with the Sahara as the emission sources [6]. At these periods of the year, high aerosol optical depth (AOD) values associated with a frequency of dust occurrences are measured at several stations of the AERONET network in the Sahel [1, 8]. To this end, a dust fall starting on July 3, 2010 from the Sahara Desert in Southern Algeria following a severe thermal depression, led to the increase in the AOD with daily average values ranging from 3.5 to 4 measured on the station of Dakar, Senegal, on July 07, 2010 [4]. In addition, a study conducted by Senghor et al [9] shows a high seasonal variability of dust layer in the West Africa zone. This enables to locate aerosols around 3 km of altitude in Spring then between 3 and 5 km in Summer. However, in Winter, dust is more noticed on the surface below 2 km [4, 9], which is source of several cases of respiratory diseases and meningitis epidemics observed during the Harmattan in the Sahel [10, 11, 12, 13]. This distribution of particles goes along with their radiative impact noticed on the surface, in the atmosphere and at the top of the atmosphere [14]. In the Sahel, atmospheric particles are strongly dominated by mineral dust characterized by their diffusion properties and absorption of solar radiation. Therefore, a reduction of direct radiation by approximately 200-300 W/m² is obtained by Dramé et al. [4] with an increase in diffuse flows from 50 W/m² to 150W/m² on the Site of Dakar in Senegal. Another study carried out on the same site in 2012 revealed a reduction by nearly 10% and 28%, respectively on the overall and direct radiation due to the effect of aerosols [15] with a solar potential calculated at 7 kWh/m²/d in May. Indeed, the African continent is one of the largest solar deposits in the world where maximum sunshine is observed in deserts, particularly the Northern part (the Sahel and the Sahara) and the Southern part (Kalahari) [16]. To this end, a study conducted by the National Aeronautics and Space Administration (NASA) between 1983 and 2005 in the Sahara ranks 2 the Agadem region in Niger as the 2nd sunniest region in the world with an average annual irradiation of 6.92 kWh/m²/d [17]. Average monthly sunshine values measured around 7 kW/m² and 8.25 kW/m² are obtained on the sites of Dakar, in Senegal and Nouakchott, in Mauritania [18]. Similarly, an evaluation of solar potential between 2015 and 2016 in Niamey shows a high availability of sunshine associated with average values between 5.1 kW/m² and 6.3 kW/m² [19]. It should also be noted that knowing the potential of solar energy for a given site is a very important for the development of scientific, technological and economic research on solar systems [17, 19]. However, much of this radiation is mitigated by the atmosphere, either by absorption, or spreading by aerosols, greenhouse gases, molecules and steam. The objective of this study is to assess the impact of aerosols on solar radiation in the Sahelian zone in Burkina Faso. The study is based on in-situ measurements from National Meteorological Agency (ANAM) stations, satellite observations and a radiative transfer model on three sites in 2017, with the objective to contribute to a better optimization of solar thermal and photovoltaic systems that constitute an alternative to meet energy deficit in this part of the Sahel.

## 2. MATERIAL AND METHODS

### 2.1 The Streamer code for radiative transfer

UNDER PEER REVIEW

The streamer code developed by Key and Schweiger (1998) and Key (2001) is a simple and fast model for assessing the radiative impact of atmospheric aerosols. In this model, the terms of the radiative budget are treated separately at different spectral bands. This is incident solar radiation calculated at wavelengths ranging from 0.4 to 0.8 microns contained in the visible spectrum and telluric infrared radiation between 0.8 and 500 microns. Indeed, the Streamer code calculates luminances and flows by cutting the atmosphere in several layers in all directions. These quantities are calculated on narrow bands and on the entire solar spectrum, then for 25 atmosphere levels distributed between the surface and the top of the atmosphere. This code uses six (06) predefined aerosol models under the terms tropospheric, marine, rural, arctic haze, smoke and urban aerosol to simulate radiation on the surface. These models were created using a Mie code that enables to generate the optical parameters of the particle. Thus, each aerosol model predefined in the Streamer code contains the extinction, absorption and asymmetry coefficients of the particle considered throughout the solar spectrum. Moreover, the absorption of the main gases ($H_2O$, $O_3$, $CO_2$, $O_2$) in the visible spectrum is included but, it can be omitted in calculations. The surface can be considered as a Lambertian one with or without isotropic reflection through its bidirectional reflectance distribution function [20]. For our study, the tropospheric model is used considering the nature of dominating particles in the Sahel, especially in Burkina Faso. Also, for the simulation of surface level solar flows, the model must be thoroughly and accurately completed [21]. For this, we use AERONET reversal data [22, 23, 24, 25, 26] and satellite observations available on NASA's Giovanni site.

## 2.2 MODIS (MODerate Resolution Imaging Spectroradiometer)

MODIS is a sensor transported by the TERRA satellites since December 1999 and Aqua in April 2002. TERRA sweeps the Earth surface from the North to the South around the equator in the morning around 10:30 am while Aqua occurs in the evening, around 10:30 am in an orbit oriented South-North of the Equator [27]. MODIS has 36 spectral bands that enable it to provide measurements on the atmosphere, the Earth and the ocean, 7 of which are used to study aerosols (466, 553, 644, 855, 1243, 1632 and 2119 nm). In addition, it uses different algorithms to invert aerosol properties on Earth [28] and on seas [29] where measurements are made with a spatial resolution ranging from 1 to 250 km and temporal from 1 to 2 days. For our study, we use MODIS-Terra and MODIS-Aqua Deep-Blue inversions at 550 nm and available on NASA's Giovanni site (https://giovanni.gsfc.nasa.gov/giovanni/). Indeed, the Deep Blue algorithm takes into account cloud masks, the aerosol model and the reflection of shiny surfaces [27, 30]. This makes it possible to eliminate contaminations due to the reflection of the shiny surfaces and to improve the qualified observations in level 2 in areas like the desert of the Sahara, the arid, semi-arid and urban regions where reflectivity is very significant [31].

## 2.3 Study Area and Sites

UNDER PEER REVIEW

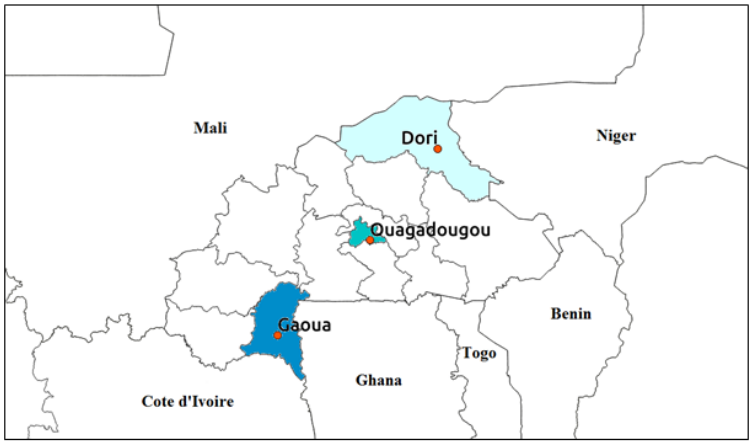


**Figure. 1.** Geographical location of the site of Dori in the North, the site of Ouagadougou in the Centre and that of Gaoua in the South of Burkina Faso.

Burkina Faso is a Sahelian country located at the heart of West Africa between latitudes 9°20 and 15° North and longitudes 5°30 West and 2°30 East. Its climate spreads over three climatic zones, including the Sahelian zone which covers the entire Northern part, a larger Sudano-Sahelian zone extending from the West to the East and a wetter Sudanian zone in the South [32]. It should also be noted that all these areas are characterized by the same wind regime, namely the Monsoon which lasts nearly four (04) months from June to September and the Harmattan, which extends from October to May. Because of its geographical location, Burkina Faso shares the same border with six States (Figure 1), including Mali and Niger in its Northern part and which are largely affected by the Sahara Desert, then Cote d'Ivoire, Ghana, Togo and Benin in the South. Thus, the study sites considered, namely that of Dori (14.035°N, -0.034°E), Ouagadougou (12.20°N, -1.40°E) and Gaoua (10.29°N, -3.25°E) are chosen according to Burkina Faso various climatic zones. Each site is identified by its geographic coordinates represented by a red dot as shown in Figure 1. These sites host each a station of the National Meteorological Agency for in-situ measurements of meteorological parameters such as solar radiation continuously available for the whole year 2017. Indeed, this concerns daily measurements made at an interval of 15 minutes between 00 hours and 23h 45 minutes and for all the days of the year 2017. The different colors, i.e. light blue, dark blue and very dark blue indicate the Sahelian, Sudano-Sahelian and Sudanian zones, respectively [32].

## 2.4 Assessment of Solar Radiation on an Horizontal Plan

The solar radiation available on a horizontal plan is given by the following equation (1) [17, 18]:

$$I = 1370 \exp\left( -\frac{TL}{\left(0.9 + 9.4 \sin\left(\gamma\right)\right)} \right) \quad (1)$$

TL is the Link cloud factor that can be calculated by the relation (2) and $\gamma$, the sun height.

$$TL = 2.4 + 14.6\beta + 0.4\left(1 + 2\beta\right)\ln\left(P_V\right) \quad (2)$$

$\beta$ is the air trouble coefficient that takes the following values depending on the areas:

$\beta = 0.05$ in rural area ;

$\beta = 0.1$ in urban area ;

$\beta = 0.2$ in industrial and polluted area.

UNDER PEER REVIEW

$P_V$ is the partial steam pressure expressed in mmHg and given by the expression (3) below:

$$P_V = \frac{760}{101325}\left(P_{at} - P_{\sec}\right) = 0.0075\left(P_{at} - P_{\sec}\right) \quad (3)$$

In this expression, $P_{at}$ refers to the atmospheric pressure in Pascal and $P_{\sec}$ the dry air pressure with $P_{\sec} = 1.01222 \times 10^5\, Pa$.

Sun height is the angle between the direction of the sun and the horizontal plane. It varies from 0° to 90° towards the zenith and from 0° to -90° towards the nadir and is then calculated by:

$$\sin\left(\gamma\right) = \sin\left(\theta\right)\sin\left(\delta\right) + \cos\left(\theta\right)\cos\left(\delta\right)\cos\left(\omega\right) \quad (4)$$

In this equation, $\theta$ is the latitude of the area, $\delta$ the solar declination which is the angle that makes the distance earth-sun compared to the equatorial plane given by the expression (5) where $n$ corresponds to day number in the year, from January 1 and $\omega$ the hour angle calculated according to the actual solar time $\left(TSV\right)$ [18, 28]:

$$\delta = 23.45\sin\left(\frac{360}{365}\left(n + 284\right)\right) \quad (5)$$

$$\omega = 15\left(TSV - 12\right) \quad (6)$$

Actual solar time is equal to the legal time $\left(Tl\right)$ corrected by an offset due to the gap between the longitude of the area and the reference longitude [17].

$$TSV = Tl - DE + \frac{\left(Et + 4\varphi\right)}{60} \quad (7)$$

$DE$ represents the time gap, $\varphi$ the longitude of the area and *Et* is the time equation in minutes.

$$Et = 9.9\sin\left[2\left(0.986 \times n + 100\right)\right] - 7.7\sin\left(0.986 \times n - 2\right) \quad (8)$$

Direct and diffuse solar irradiances on a horizontal plane are given by formulas (9) and (10), respectively.

$$I_b = I \cdot \sin\left(\gamma\right) \quad (9)$$

$$I_d = 54.8\sqrt{\sin\left(\gamma\right)} \cdot \left[TL - 0.5 - \sqrt{\sin\left(\gamma\right)}\right] \quad (10)$$

Thus, the overall illumination $I_g$ on a horizontal plane is the sum of direct and diffuse radiation where:

$$I_g = I_b + I_d \quad (11)$$

The overall solar radiation is measured on the various sites by the meteorological stations and the solar energy potential available on a horizontal plane $\left(E_g\right)$ is calculated from the equation (12) following the sunrise (SR) and the sunset (SS) [15].

$$E_g = \int_{Ls}^{Cs} I_g\left(t\right)dt \quad (12)$$

UNDER PEER REVIEW

## 3. RESULTS AND DISCUSSION

### 3.1 Time Variability of the Sun Energy Potential

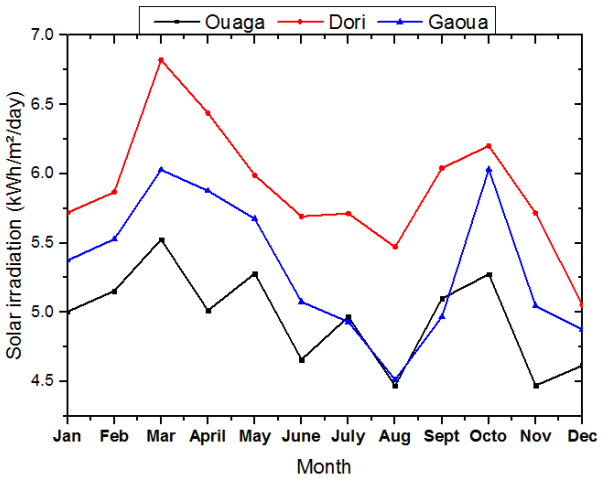


**Figure. 2.** Monthly average of the overall solar potential in (kWh/m²/d) in Ouagadougou, Dori and Gaoua sites in 2017

Figure 2 shows the evolution of solar potential available in Burkina Faso through in-situ measurements at the sites of Ouagadougou, Dori and Gaoua. The analysis of this figure shows a very great variability of the solar potential measured [15, 16], especially on the station of Ouagadougou with a high potential of solar energy available on the Dori site followed by that of Gaoua. The maxima are all observed in Spring in March and in Autumn in October probably due to a strong solar activity due to isolation time over these periods of Harmattan. However, the minimum sunshine is observed in Summer, in August because of the rainy season and cloud cover, then in Winter, in December, characterized by low isolation time of sunshine. This corresponds to a monthly average of solar irradiation varying between 5.05 kW/m²/d to 6.82 kW/m²/d, 4.51 kW/m²/d to 6.03 kW/m²/d and 4.46 kW/m²/d to 5.52 kW/m²/d calculated on the sites of Dori, Gaoua and Ouagadougou, respectively. Thus, this high potential of solar energy available is clearly shown by average monthly values of solar energy ranging between 4.46 kW/m²/d and 6.82 kW/m²/d, of which the most favorable months are March (Spring) and October (Fall) while the adverse period is in August (Summer) and December (winter). Indeed, Dori is a city located in the Northern part of Burkina Faso at the heart of the Sahel considered to be one of the sunniest areas on the African continent. On the other hand, Gaoua is a city located in the South-West with a humid tropical climate and may be characterized by an atmosphere under the weak influence of desert dust, notably during the dry season, in Autumn, Winter and Spring. As for Ouagadougou located in the Center, sunshine level can be affected by a more polluted atmosphere given the high population density and socio-economic activities. Additionally, Ouagadougou may be under the influence of North-East winds, responsible of dust and South-West winds that cause the rise of combustion particles toward the North [1, 2, 8], creating a plume of aerosols on this site.

UNDER PEER REVIEW

### 3.2 Qualitative evolution of aerosols compared to solar energy potential

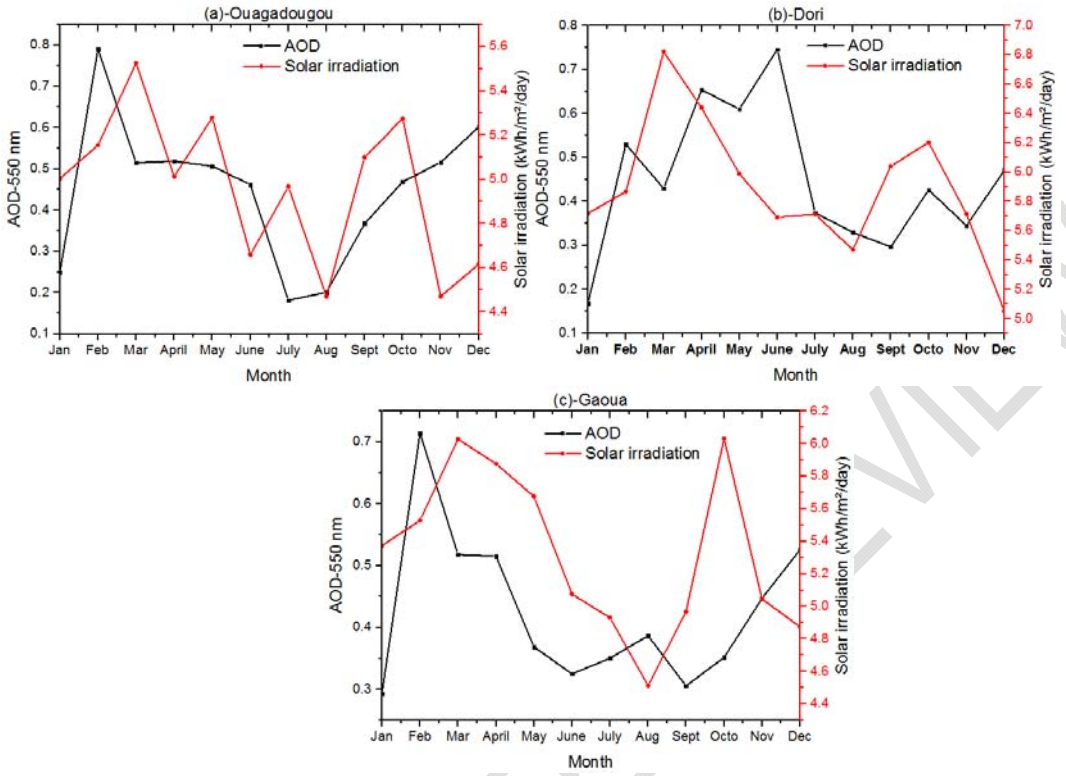


**Figure. 3.** Monthly average of the AOD at 550 nm and of the solar potential in Ouagadougou, Dori and Gaoua sites in 2017

Figure 3 is drawn to show the impact of aerosols on solar potential. It illustrates the evolution of solar energy measured at these three stations with the reverse aerosol optical depth (AOD) in the MODerate Resolution Imaging Spectroradiometer (MODIS) blue channel [29, 30] at 550 nm. Therefore, it should be noticed that the peak of solar potential in March corresponds to a minimum of AOD for all sites. A similar observation is also made in July in Ouagadougou and September-October in Gaoua. On the other hand, the maximum AOD in February is clearly associated with a minimum solar potential. It is the same for June and November on the Ouagadougou site, June in Dori and August for Gaoua site. This variability of the potential and the AOD clearly shows a significant role played by aerosols in the mitigation of solar radiation at the crossing of the atmosphere up to the surface of the Earth. This could be in agreement with solar potential fluctuations observed on all the sites, notably on that of Ouagadougou characterized by a great variability. This impact of the aerosols will be quantified later with the Streamer model of radiative transfer previously described. However, the minimum solar irradiation during rainy periods (June, July, August and September) is due to rainfall and cloud cover [15].

### 3.3 Frequency calculations and day classification

UNDER PEER REVIEW

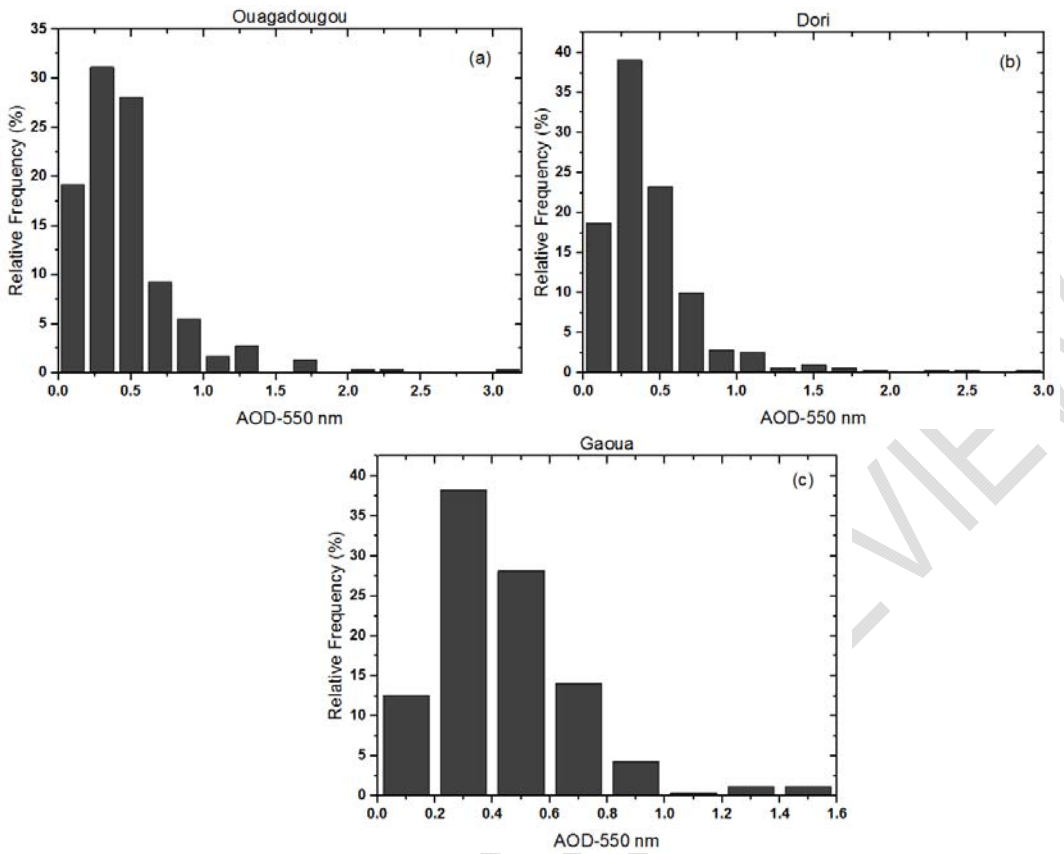


**Figure. 4.** Frequency distribution of AOD daily averages at 550 nm in Ouagadougou, Dori and Gaoua in 2017

For a better distribution of days following the atmospheric aerosol load, a daily AOD frequency distribution 550 nm of the MODIS-Terra and Aqua sensor is performed and presented in figure 4. This will enable to see later on the impact of aerosols on the solar potential depending on the particulate filer of the atmosphere. Following this, we find that most days observed on all sites are defined by AOD values ranging between 0.2 and 0.8 corresponding to nearly 88% of days for the Ouagadougou site (Figure 4a), 91% in Dori site (Figure 4b) and 93% for that of Gaoua (Figure 4c). In addition, the maximum frequency is around 0.4 and represents 31.16%, 39.03% and 38.28% for the sites of Ouagadougou, Dori and Gaoua, respectively. This is the frequency of standard days characterized by moderately polluted conditions that are the most observed [34]. However, days with AOD ≥ 1 are less frequent and are associated with a highly polluted atmosphere with dust events illustrated by AOD ≥ 2. Based on frequency analysis and in line with Dramé et al [34], Dérimian et al [35], we classify days into three categories: clear-sky days characterized by AOD values less than 0.2, mixed days with AOD values ranging between 0.2 and 0.8 and polluted days corresponding to AOD higher than 0.8 (AOD > 0.8). As shown in Figure 4, mixed or intermediate days are the most frequent and are due to a mixture of dust and combustion particles. They also concern the standard days (AOD = 0.4) which dominate this category of days and characterized by a medium pollution of the atmosphere. At the end of this classification, days chosen for our study are recorded in Table 1 below.

**Table. 1.** Summary of the days chosen on the various sites for the assessment of aerosols impact

| Dori | | | Ouagadougou | | | Gaoua | | |
|---|---|---|---|---|---|---|---|---|
| Date | AOD | Day | Date | AOD | Day | Date | AOD | Day |
| 28/09/2017 | 0.17 | Clear | 01/12/17 | 0.09 | Clear | 25/01/17 | 0.14 | Clear |
| 16/12/2017 | 0.60 | Mixed | 26/12/17 | 0.82 | Mixed | 26/12/17 | 0.84 | Mixed |
| 04/02/2017 | 2.53 | Polluted | 09/12/17 | 3.09 | Polluted | 05/02/17 | 1.61 | Polluted |

## 3.4 Simulation of solar radiation and assessment of aerosols impact

### 3.4.1 Impact of aerosols on solar radiation at Dori

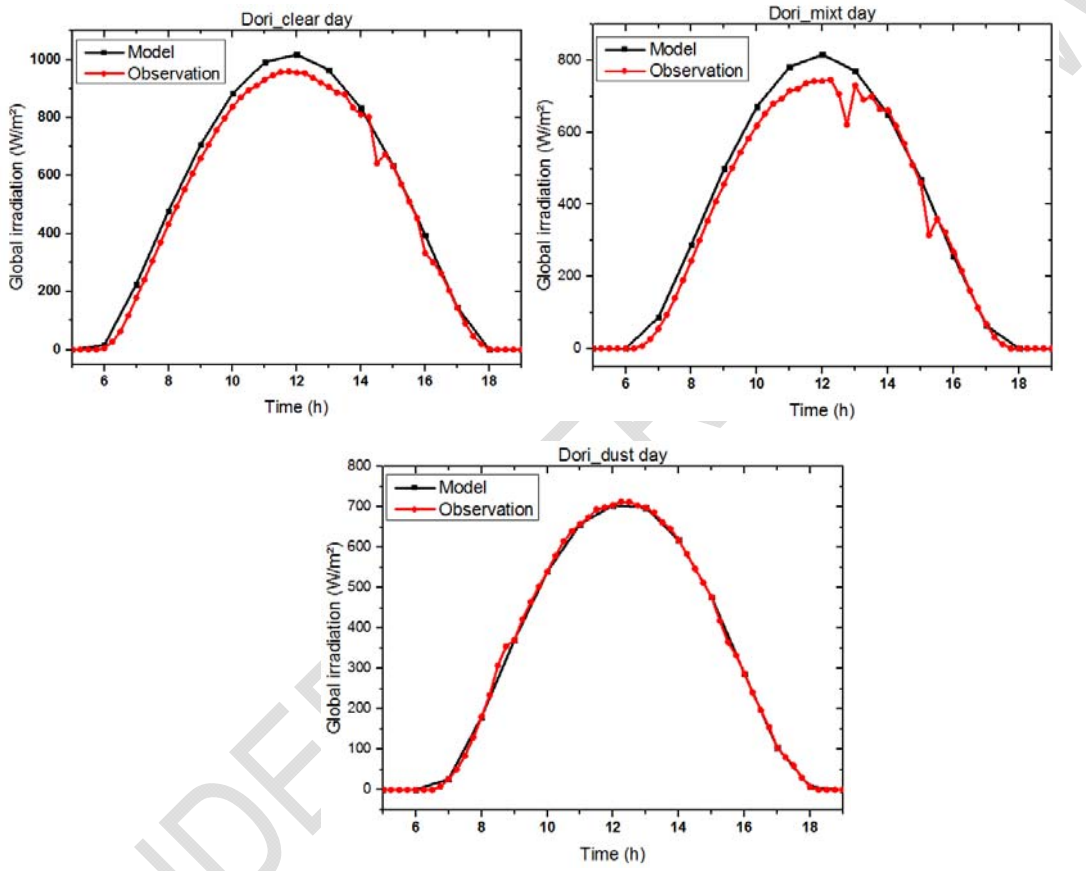


**Figure. 5.** Simulation of the overall solar radiation at Dori station

The impact of aerosols on radiation is difficult to observe through the overall flow at the surface which is the sum of the flow mitigated by diffusion or absorption and normal direct. However, to better assess their effect, we made a simulation of the overall radiation of the day illustrated by day cycles in Figure 5 in the case of cloudless standard atmosphere. This enables us to adjust the simulated overall radiation with that of the observation made on the site and then to obtain the corresponding direct and diffuse radiation. Moreover, this comparison between the overall solar flow of the model and the in-situ measurement shows good accuracy of the Streamer model to estimate solar radiation at surface level [20] in Burkina Faso, particularly in the North.

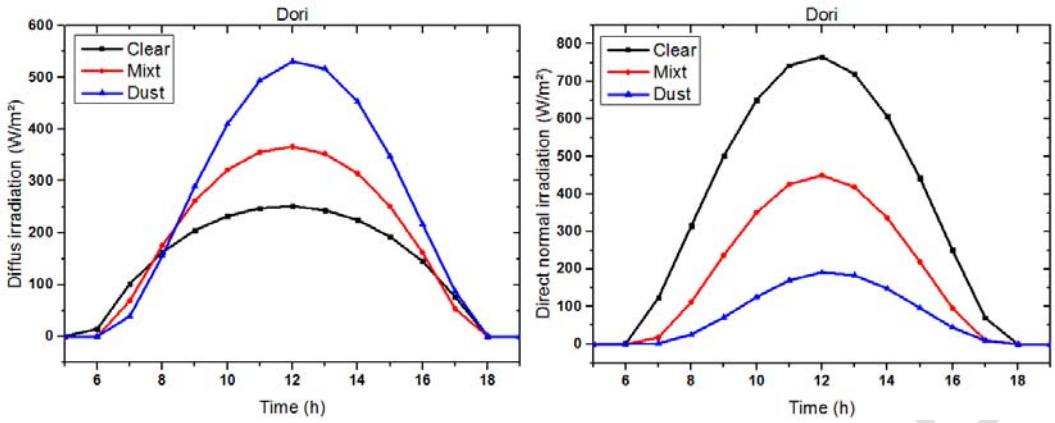


**Figure. 6.** Simulation of normal diffuse and direct solar radiation at Dori station

Figure 6 shows the day evolution of the normal diffuse and direct solar radiation on Dori site following the concentration of particles defined by clear, mixed and polluted days. We find that the diffuse flow increases with the optical thickness and varies from 251.39 W/m² to 366.43 W/m², going from the clear day (AOD = 0.17) to the mixed one (AOD = 0.60). This variation is from 251.39 W/m² to 531.08 W/m² for clear days and polluted days (AOD = 2.53). Thus, an increase by 279.69 W/m² is obtained in this dusty day against 115.04 W/m² for the mixed day characterized by a moderately loaded atmosphere in aerosols. However, the normal direct considerably descreases as the AOD increases. In fact, the maximum direct solar flow obtained is 766.37 W/m², 450.19 W/m² and 191.21 W/m², respectively, during clear, mixed and polluted days. This corresponds to a decrease of nearly 41.25% and 75.04% of normal direct flow calculated during the mixed and polluted day respectively compared to the clear day at the Dori site in the Northern par of Burkina Faso, under the strong influence of the Sahel and the Sahara. This energy loss on this polluted day of February 4, defined by AOD equals to 2.53 is clearly due to desert dust characterized by a strong diffusion of solar radiation [1, 15].

### 3.4.2 Impact of aerosols solar radiation in Ouagadougou

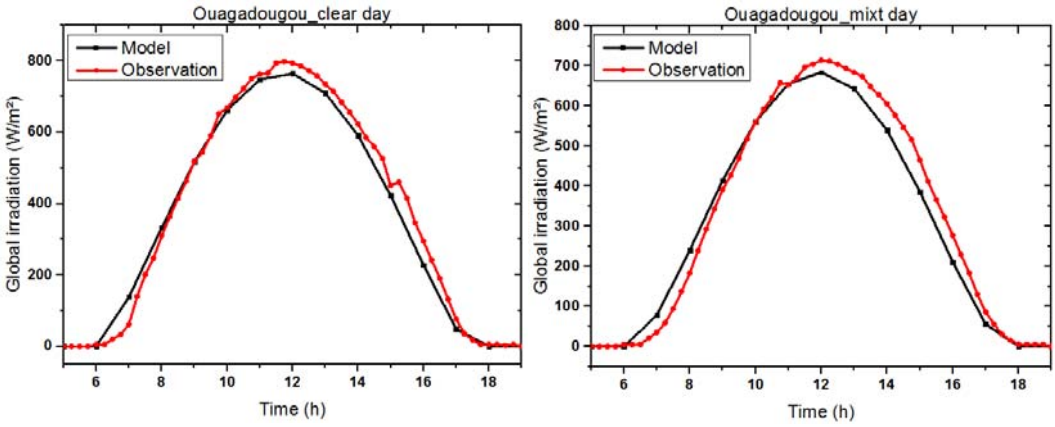

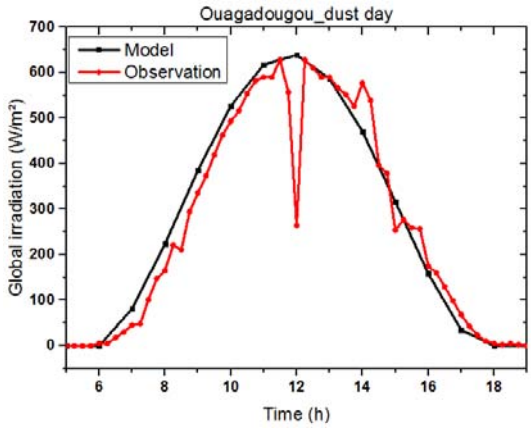


**Figure. 7.** Simulation of the overall solar radiation at the Ouagadougou station

The overall radiation simulated and compared to the in-situ measurements is presented in Figure 7. Therefore, we got a good estimate of observations made in Ouagadougou, which corresponding normal diffuse and direct sunlight and associated with each type of day is clearly shown in figure 8. Its analysis shows a similar evolution of the diffuse and the normal direct according to the atmospheric load in aerosols previously noticed on the site of Dori. However, the diffuse observed on the Ouagadougou site goes from 267.97 W/m² for the clear day (AOD = 0.09) to 418.40 W/m², then to 514.02 W/m², respectively for the mixed day (AOD = 0.82) and polluted (AOD = 3.09). The increase noticed for the clear day is estimated at 150.43 W/m² and 246.05 W/m², respectively during the mixed day characterized by a plume of mineral aerosols and combustion particles and polluted due to dust [34, 35].

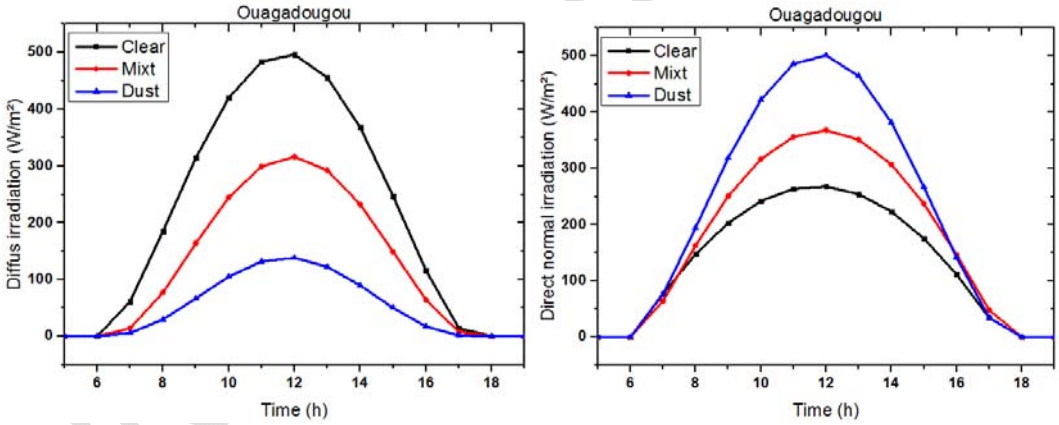


**Figure. 8.** Simulation of the diffuse and direct normal radiation on the Ouagadougou station

At the same time, the normal direct undergoes a reverse evolution with a loss of the direct solar flow of nearly 22.11% and 57.33% during mixed and polluted days, respectively. Indeed, the maximum direct solar radiation calculated for these clear, mixed and polluted days is 496.39 W/m², 386.63 W/m² and 211.78W/m², respectively.

### 3.4.3 Impact of aerosols solar radiation at Gaoua

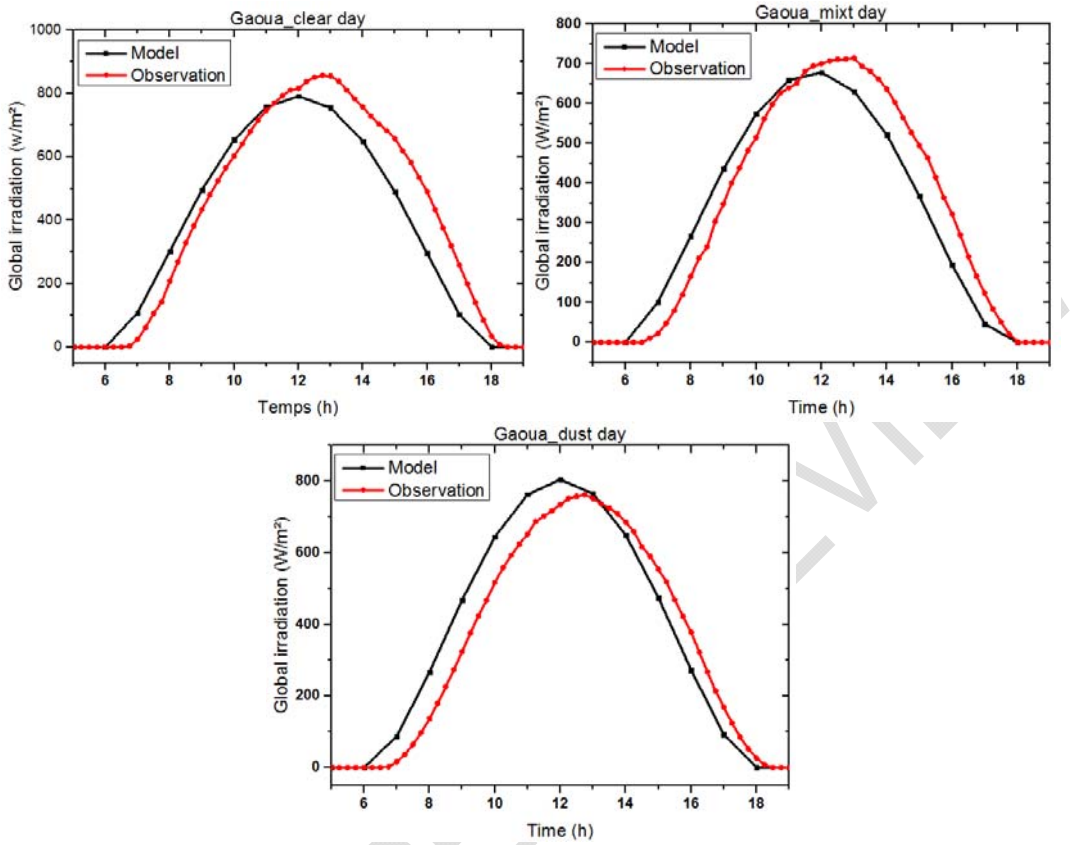


**Figure. 9.** Simulation of global solar radiation at Gaoua station

A simulation of the overall radiation compared to the observations made on Gaoua site (figure 9) gives like for Ouagadougou and Dori, the precision of the model in the calculation of the solar flow in this southern part of the country. Following this, we obtain a separation of the solar flow into diffuse and direct normal components observed in Figure 10.

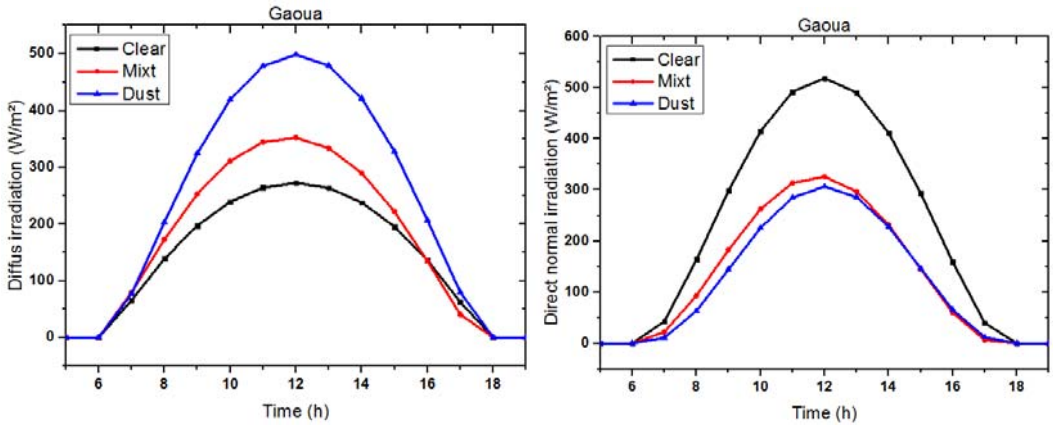


**Figure. 10.** Simulation of diffuse and direct normal solar radiation on Gaoua station

An analysis of this figure indicates the same remarks made on the day evolution of the diffuse and direct normal radiation on the two previous sites. Indeed, on the Gaoua site, the diffuse flow increases according to days characterzied by AOD values and this variation is 79.58 W/m² and 226.09 W/m² going from a clear day (AOD = 0.14) to a mixed day (AOD = 0.84) or polluted day (AOD = 1.61), respectively. This corresponds to a maximum of diffuse radiation noticed at 272.37 W/m² for a clear day, 351.95 W/m² for a mixed day and 498.46 W/m² during the polluted day. Normal direct flow follows a reverse diffuse flow variation when AOD increases. Thus, compared to the clear day, a loss of 37.13% and 40.89% of this flow are recorded respectively during the mixed and polluted days in Gaoua, with a maximum of normal direct flow calculated at 518.88 W/m² for a clear day, 326.19 W/m² under mixed day and 306.70 W/m² for a highly polluted atmosphere.

## 4. CONCLUSION

This study involved evaluating the impact of aerosols on the solar energy potential available from a Streamer radiative transfer code. In this respect, an assessment of the solar potential based on the in-situ measurements from meteorological stations located on Dori, Ouagadougou and Gaoua sites is made. This shows a high potential of solar energy in Burkina Faso, notably in its Northern part and characterized by monthly average values between 4.46 kW/m²/d and 6.82 kW/m²/d. However, a qualitative analysis between the aerosol cycle and this potential shows the major role of atmospheric particles in mitigating day radiation with minima or maxima of the potential associated with the AOD maxima or minima. In addition, the quantification of aerosols impact using the standard tropospheric model of the Streamer code reveals a decreases in the normal direct flow followed by a large increase in diffuse flow as the aerosol optical depth (AOD) increases. This decrease in the normal direct flow is estimated at nearly 75.04% on the site of Dori in the North, at 57.33% on that of Ouagadougou in the Center and at 40.89% on the site of Gaoua located in the South of the country during polluted days corresponding to AOD higher than 0.8 (AOD > 0.8). These energy losses are estimated, compared to clear days characterized by aerosol optical depth (AOD) less than 0.2.

## ACKNOWLEDGEMENTS

We thank Didier, the principal investigator of AERONET sites for the availability of AERONET data and NASA (National Aeronautics and Space Administration) for earth observations. We are further thankful to the Agence Nationale de la Météorologie du Burkina-Faso (ANAM). The ISP, Uppsala University, Sweden is gratefully acknowledged for their support to project BUF01.

## REFERENCES

[1] B. Nébon, M. S. Dramé, K. Bruno, K. P. Florent, S. M. Sall, and D. Joseph, “Optical and microphysical analysis of aerosols in Sahelian Zone : Case of the Ouagadougou City in Burkina Faso,” *Elixir Int. J.*, vol. 119, pp. 50975–50982, 2018.

[2] S. Woodward, “Modeling the atmospheric life cycle and radiative impact of mineral dust in the Hadley Centre climate mode,” *J. Geophys. Res.*, vol. 106, no. 2000, pp. 18155–18166, 2001.

[3] Guillaume A. D’Almeida, “A model for Saharan dust transport,” *Am. Meteorol. Soc.*, vol. 25, pp. 903–916, 1986.

[4] M. Drame, G. S. Jenkins, M. Camara, and M. Robjhon, “Observations and simulation of a Saharan air layer event with a midtropospheric dust layer at Dakar , Senegal , 6 – 7 July 2010,” *J. Geophys. Res.*, vol. 116, pp. 6–7, 2011.

[5] J. Huang, P. Minnis, H. Yan, Y. Yi, B. Chen, L. Zhang, and J. K. Ayers, “Dust aerosol effect on semi-arid climate over Northwest China detected from A-Train satellite measurements,” *Atmos. Chem. Phys.*, pp. 6863–6872, 2010.

[6] J. M. Prospero, P. Ginoux, O. Torres, S. E. Nicholson, and T. E. Gill, “Environmental characterization of global sources of atmospheric soil dust identified with the nimbus 7 total

UNDER PEER REVIEW

ozone mapping spectrometer (TOMS) absorbing aerosol product," *Rev. Geophys.*, vol. 40, no. February, pp. 1–31, 2002.
[7] Z. Li, X. Xia, M. Cribb, W. Mi, B. Holben, P. Wang, H. Chen, S. Tsay, T. F. Eck, F. Zhao, E. G. Dutton, and R. E. Dickerson, "Aerosol optical properties and their radiative effects in northern China," *J. Geophys. Res.*, vol. 112, no. April, pp. 1–11, 2008.
[8] M. S. Drame, M. Camara, and A. T. Gaye, "Intra-Seasonal Variability of Aerosols and Their Radiative Impacts on Sahel Climate during the Period 2000-2010 Using AERONET Data," *Int. J. Geosci.*, vol. 4, pp. 267–273, 2013.
[9] H. Senghor, É. Machu, F. Hourdin, and A. T. Gaye, "Seasonal cycle of desert aerosols in western Africa : analysis of the coastal transition with passive and active sensors," *Atmos. Chem. Phys.*, vol. 17, pp. 8395–8410, 2017.
[10] R. J. Delfino, C. Sioutas, and S. Malik, "Review Potential Role of Ultrafine Particles in Associations between Airborne Particle Mass and Cardiovascular Health," *Environ. Health Perspect.*, vol. 113, no. 8, pp. 934–946, 2005.
[11] K. Donaldson, V. Stone, A. Seaton, and W. Macnee, "Ambient Particle Inhalation and the Cardiovascular System : Potential Mechanisms," *Environ. Health Perspect.*, vol. 109, no. 4, pp. 523–527, 2001.
[12] B. Sultan, K. Labadi, J.-F. Guégan, and S. Janicot, "Climate Drives the Meningitis Epidemics Onset in West Africa," *Plos Med.*, vol. 2, no. 1, pp. 0043–0049, 2005.
[13] A. M. Diokhane, G. S. Jenkins, N. Manga, and M. S. Drame, "Linkages between observed , modeled Saharan dust loading and meningitis in Senegal during 2012 and 2013," *Int J Biometeorol*, pp. 557–575, 2015.
[14] B. Korgo, "Caractérisation optique et microphysique des aérosols atmosphériques en zone urbaine ouest africaine : application aux calculs du forçage radiatif à Ouagadougou," Universite de Ouagadougou, 2014.
[15] M. Drame, B. O. Bilal, M. Camara, V. Sambou, and A. Gaye, "Impacts of aerosols on available solar energy at Mbour , Senegal," *J. Renew. Sustain. Energy*, vol. 4, pp. 1–13, 2012.
[16] M. S. Drame, "Caractérisation et impacts climatiques des aérosols en Afrique de l'ouest," Université Cheick Anta DIOP de Dakar, 2012.
[17] M. Dankassoua, S. Madougou, and A. A. A. Foulani, "Etude du rayonnement solaire global à Niamey de la période de pré- mousson et de la mousson de l ' année 2013 ( mai à octobre )," *Rev. des Energies Renouvelables*, vol. 20, pp. 131–146, 2017.
[18] B. O. Bilal, V. Sambou, C. M. F. Kébé, M. Ndongo, and P. A. Ndiaye, "Etude et modélisation du potentiel solaire du site de Nouakchott et de Dakar," *J. des Sci.*, vol. 7, pp. 57–66, 2007.
[19] M. Dankassoua, M. Saïdou, and S. Yahaya, "Evaluation of Solar Potential at Niamey : Study Data of Insolation from 2015 and 2016," pp. 394–411, 2017.
[20] M. S. Drame, M. Camara, and A. T. Gaye, "Simulation de l ' impact des aérosols sur le rayonnement solaire à Mbour , Sénégal," *La Météorologie*, pp. 51–57, 2012.
[21] V. Camille, "Etude de l'impact radiatif des aérosols dans la couche limite planetaire," Université de Versailles, 2007.
[22] B. N. Holben, T. F. Eck, I. Slutsker, D. Tanre, J. P. Buis, A. Setzer, E. Vermote, J. A. Reagan, Y. J. Kaufman, T. Nakajima, F. Lavenu, I. Jankowiak, and A. Smirnov, "AERONET — A Federated Instrument Network and Data Archive for Aerosol Characterization," *Remote Sens. Environ.*, vol. 4257, no. 98, pp. 1-16, 1998.
[23] O. Dubovik, "Optimization of numerical inversion in photopolarimetric remote sensing," *Kluwer Acad. Publ. Print. Netherlands*, pp. 65–106, 2004.
[24] O. Dubovik and D. King, "A flexible inversion algorithm for retrieval of aerosol optical properties from Sun and sky radiance measurements,"*J. Geophys. Res.*, vol. 105, pp. 20673–20696, 2000.
[25] O. Dubovik, A. Smirnov, B. N. Holben, M. D. King, Y. J. Kaufman, T. F. Eck, and I. Slutske, "Accuracy assessments of aerosol optical properties retrieved from Aerosol Robotic Network ( AERONET ) Sun and sky," *Geophys. Res.*, vol. 105, no. D8, pp. 9791–9806,

UNDER PEER REVIEW

2000.
[26] O. Dubovik, B. N. Holben, T. Lapyonok, A. Sinyuk, M. I. Mishchenko, P. Yang, and I. Slutsker, “Non-spherical aerosol retrieval method employing light scattering by spheroids,” *Geophys. Res. Lett.*, vol. 29, no. 10, pp. 3–6, 2002.
[27] R. C. Levy, L. A. Remer, S. Mattoo, E. F. Vermote, and Y. J. Kaufman, “Second-generation operational algorithm : Retrieval of aerosol properties over land from inversion of Moderate Resolution Imaging Spectroradiometer spectral reflectance,” *J. Geophys. Res.*, vol. 112, pp. 1–21, 2007.
[28] Y. J. Kaufman, D. Tanr, L. A. Remer, E. F. Vermote, and A. Chu, “Operational remote sensing of tropospheric aerosol over land from EOS moderate resolution imaging spectroradiometer After the launch of MODIS the distribution,” *J. Geophys. Res.*, vol. 102, no. 96, pp. 51–67, 1997.
[29] D. Tanré, Y. J. Kaufman, M. Herman, and S. Mattoo, “Remote sensing of aerosol properties over oceans using the MODIS / EOS spectral radiances,” *J. Geophys. Res.*, vol. 102, no. 3, pp. 16971-16988, 1997.
[30] L. A. Remer, Y. J. Kaufman., D. Tanré, S. Mattoo, D. A. Chu, J. V. Martins, R. R. Li, C. Ichoku, R. C. Levy, R. G. Kleidman, T. F. Eck, E. Vermote, and B. N. Holben, “The MODIS Aerosol Algorithm, Products, and Validation,” *Am. Meteorol. Soc.*, vol. 62, pp. 947–973, 2005.
[31] N. C. Hsu, S. Tsay, M. D. King, S. Member, and J. R. Herman, “Aerosol Properties Over Bright-Reflecting Source Regions,” *IEEE Trans. Geosci. Remote Sens.*, vol. 42, no. 3, pp. 557–569, 2004.
[32] B. Kabore, S. Kam, G. W. P. Ouedraogo, and D. J. Bathiébo, “Etude de l’évolution climatique au Burkina Faso de 1983 à 2012 : cas des villes de Bobo Dioulasso, Ouagadougou et Dori,” *Arab. J. Earth Sci.*, vol. 4, no. 2, pp. 50–59, 2017.
[33] K. Kerkouche, F. Cherfa, A. H. Arab, S. Bouchakour, K. Abdeladim, and K. Bergheul, “Evaluation de l ’ irradiation solaire globale sur une surface inclinée selon différents modèles pour le site de Bouzaréah,” *Rev. des Energies Renouvelables*, vol. 16, pp. 269–284, 2013.
[34] M. S. Drame, X. Ceamanos, J. L. Roujean, A. Boone, J. P. Lafore, D. Carrer, and O. Geoffroy, “On the Importance of Aerosol Composition for Estimating Incoming Solar Radiation: Focus on the Western African Stations of Dakar and Niamey during the Dry Season,” *Atmosphere (Basel).*, vol. 6, pp. 1608–1632, 2015.
[35] Y. Derimian, J. Le, O. Dubovik, I. Chiapello, D. Tanre, T. Podvin, G. Brogniez, and B. N. Holben, “Radiative properties of aerosol mixture observed during the dry season 2006 over M ’ Bour , Senegal ( African Monsoon Multidisciplinary Analysis campaign ),” *J. Geophys. Res.*, vol. 113, pp. 1–15, 2008.

UNDER PEER REVIEW